Human Serum Albumin Self-Assembly on Weak Polyelectrolyte Multilayer Films Structurally Modified by pH Changes

ARTICLE *in* LANGMUIR · JULY 2004

Impact Factor: 4.46 · DOI: 10.1021/la049932x · Source: PubMed

7 AUTHORS, INCLUDING:

Csilla Gergely
Université de Montpellier
148 PUBLICATIONS **1,872** CITATIONS
SEE PROFILE

Balazs Szalontai
Hungarian Academy of Sciences
56 PUBLICATIONS **1,070** CITATIONS
SEE PROFILE

Hector Flores
Universidad Autónoma de San Luis Potosí
30 PUBLICATIONS **198** CITATIONS
SEE PROFILE

Frédéric Cuisinier
Université de Montpellier
199 PUBLICATIONS **3,208** CITATIONS
SEE PROFILE

Human Serum Albumin Self-Assembly on Weak Polyelectrolyte Multilayer Films Structurally Modified by pH Changes

Csilla Gergely,[†,‡] Sophie Bahi,[†] Balázs Szalontai,[‡] Hector Flores,[†] Pierre Schaaf,[§] Jean-Claude Voegel,[*,†] and Frédéric J. G. Cuisinier[†]

Institut National de la Santé et de la Recherche Médicale, Unité 595, Faculté de Chirurgie Dentaire, Université Louis Pasteur, 11, rue Humann, 67085 Strasbourg Cedex, France, Institute of Biophysics, Biological Research Center of the Hungarian Academy of Sciences, 6726 Szeged, Hungary, and Institut Charles Sadron, Centre National de la Recherche Scientifique, Université Louis Pasteur, 6 rue Boussingault, 67083 Strasbourg Cedex, France

Received January 8, 2004. In Final Form: April 5, 2004

Adsorption of proteins onto film surfaces built up layer by layer from oppositely charged polyelectrolytes is a complex phenomenon, governed by electrostatic forces, hydrogen bonds, and hydrophobic interactions. The amounts of the interacting charges, however, both in polyelectrolytes and in proteins adsorbed on such films are a function of the pH of the solution. In addition, the number and the accessibility of free charges in proteins depend on the secondary structure of the protein. The subtle interplay of all these factors determines the adsorption of the proteins onto the polyelectrolyte film surfaces. We investigated the effect of these parameters for polyelectrolyte films built up from weak "protein-like" polyelectrolytes (i.e., polypeptides), poly(L-lysine) (PLL), and poly(glutamic acid) (PGA) and for the adsorption of human serum albumin (HSA) onto these films in the pH range 3.0−10.5. It was found that the buildup of the polyelectrolyte films is not a simple function of the pure charges of the individual polyelectrolytes, as estimated from their respective pK_a values. The adsorption of HSA onto $(PLL/PGA)_n$ films depended strongly on the polyelectrolyte terminating the film. For PLL-terminated polyelectrolyte films, at low pH, repulsion, as expected, is limiting the adsorption of HSA (having net positive charge below pH 4.6) since PLL is also positively charged here. At high pH values, an unexpected HSA uptake was found on the PGA-ending films, even when both PGA and HSA were negatively charged. It is suggested that the higher surface rugosity and the decrease of the α-helix content at basic pH values (making accessible certain charged groups of the protein for interactions with the polyelectrolyte film) could explain this behavior.

Introduction

The alternated physisorption of oppositely charged polyions at a solid/liquid interface, introduced by Decher in 1992, constitutes a versatile and powerful assembling technique for supramolecular architectures.[1,2] The approach offers many advantages such as large freedom in construction, no hindrance of substrate size and topology, and good mechanical and chemical film stabilities. This assembling technique allows these films to be combined with particles, inorganic complexes, salts, crystals, enzymes, or proteins being deposited on the top of the film or incorporated between the polyelectrolyte layers. In particular, protein adsorption or embedding offers interesting functionalization possibilities. Alternated protein and polyelectrolyte adsorption led to mixed multilayered polyelectrolyte/protein architectures.[3,4] Such constructions could be used as enzyme reactors, and it was shown that multilayer films of glucose-oxidase and peroxidase[5] and glucose-amylase and glucose-oxidase[6] permitted cascades of enzymatic reactions. Immunosensing measurements on inserted anti-immunoglobulin G (anti-Ig G) showed additive affinity for IgG's until fewer than four polyelectrolyte layers were deposited onto the protein.[7]

More recently, it was shown that proteins may adsorb on either positively or negatively charged polyelectrolyte-terminated films.[8,9] However, the thickness of the protein layer and the amount of the uptaken protein varied largely with the ionic strength and with the charge difference between the adsorbed protein and terminating film layer. This clearly showed the electrostatic origin of the interactions governing adsorption. For human serum albumin (HSA), it was demonstrated that it could be adsorbed in amounts considerably larger than needed for a monolayer.

Polyelectrolyte multilayer films can also be built using weak polyions, which render polyelectrolyte ionization largely pH dependent. In the absence of salt (i.e., at low ionic strength), strong polyelectrolytes typically deposit in thin layers, but weak polyelectrolytes exhibit large variations in layer thickness and loops and tails above or

* Corresponding author. Mail: INSERM U. 595 11, rue Humann, 67085 Strasbourg Cedex, France. Phone: +33 3 90243387. Fax: +33 3 90243379. E-mail: Jean-Claude.Voegel@medecine.u-strasbg.fr.

† Institut National de la Santé et de la Recherche Médicale, Unité 595, Faculté de Chirurgie Dentaire, Université Louis Pasteur.

‡ Institute of Biophysics, Biological Research Center of the Hungarian Academy of Sciences.

§ Institut Charles Sadron, Centre National de la Recherche Scientifique, Université Louis Pasteur.

(1) Decher, G.; Hong, J. D.; Schmitt, J. *Thin Solid Films* **1992**, *210*, 831.
(2) Decher, G. *Science* **1997**, *277*, 1232.
(3) Diederich, A.; Losche, M. *Adv. Biophys.* **1997**, *34*, 4213.
(4) Lvov, Y.; Ariga, K.; Kunitake, T. *Chem. Lett.* **1994**, *21*, 2323.
(5) Lvov, Y.; Ariga, K.; Ichinose, I.; Kunitake, T. *J. Am. Chem. Soc.* **1995**, *117*, 6117.
(6) Lvov, Y.; Decher, G.; Sukhorukov, G. *Macromolecules* **1993**, *26*, 5396.
(7) Caruso, F.; Niikura, K.; Furlong, D. N.; Okahata, Y. *Langmuir* **1997**, *13*, 3427.
(8) Picart, C.; Ladam, G.; Senger, B.; Voegel, J.-C.; Schaaf, P.; Cuisinier, F. J. G.; Gergely, C. *J. Chem. Phys.* **2001**, *115*, 1086.
(9) Ladam, G.; Gergely, C.; Senger, B.; Decher, G.; Voegel, J.-C.; Schaaf, P.; Cuisinier, F. J. G. *Biomacromolecules* **2000**, *1*, 674.

10.1021/la049932x CCC: $27.50
Published on Web 05/19/2004

below their pK_a due to incomplete charge compensation.[10] For poly(acrylic acid)/polyallylamine (PAC/PAH) films built in the absence of salts, in the pH range 4.5−5.0, where the thickness of the adsorbed layers was maximal, the surface rugosity was also strongly enhanced.[10]

In certain cases, protein adsorption on multilayers of weak polyacids exhibited antifouling properties. Müller et al.[11,12] showed very weak human fibrinogen, lysozyme, γ-immunoglobulin, and human serum albumin uptake at physiological pH conditions on a PAC-terminated film for the poly(ethyleneimine)/PAC system.

Over the past years, the achievements in multilayer assembly functionalization constituted promising approaches with respect to applications in biomaterial coatings, rendering them biocompatible. The work presented here is aimed to investigate the adsorption of proteins on multilayered polyelectrolyte films deposited on a solid surface at high (0.15 M) ionic strength and at different pH values. The step-by-step buildup of the multilayers and HSA adsorption were monitored by means of optical waveguide spectroscopy. The precursor film was realized by an initial adsorption of polyethylenimine (PEI), followed by adsorption of two alternated polystyrene sulfonate (PSS) and PAH layers. The film construction was pursued by further alternated weak polyelectrolyte poly(glutamic acid) (PGA) and poly(L-lysine) (PLL) adsorptions. The two investigated architectures were finally PEI−(PSS−PAH)$_2$−(PGA−PLL)$_3$ and PEI−(PSS−PAH)$_2$−(PGA−PLL)$_2$−PGA. Since the degree of ionization of the polypeptides is pH sensitive, it should be possible to modulate the PLL−PGA ion pairing (or electrostatic) interactions by controlling the solution's pH. This experimental parameter provides the possibility of charge alterations of both the polyanion and the polycation, giving a molecular organization that can be easily handled. Therefore film buildup and further HSA adsorption were performed at a constant ionic strength of 0.15 M, whereas pH values were varied between pH 3 and 10.5.

Atomic force microscopy was employed to visualize the surfaces and to determine the roughness of the multilayers. Conformational changes of HSA at pD values 3.0, 7.0, and 10.0 were followed by Fourier transform infrared spectroscopy.

Materials and Methods

Materials. Anionic poly(sodium 4-styrenesulfonate) (PSS, MW = 60 000), cationic poly(allylamine hydrochloride) (PAH, MW = 70 000), and cationic poly(ethyleneimine) (PEI, MW = 60 000) were purchased from Aldrich. The polypeptides poly(glutamic acid) (PGA, MW = 50 000−70 000, cat. no. 4886) and poly(L-lysine) (PLL, MW = 30 000−46 000, cat. no. 2636) were from Sigma Aldrich. NaCl (purity ≥ 99.5%) was purchased from Fluka; tris-(hydroxymethyl)-aminomethane (TRIS) and 2-(*N*-morpholino)ethanesulfonic acid (MES) were also from Sigma. All the chemicals of commercial origin were used without further purification. Ultrapure water (Milli-Q-plus system, Millipore) was used for solutions and in the different cleaning steps. All buffer solutions were degassed under a vacuum and filtered before use. The polyelectrolytes were dissolved in 25 mM MES, 25 mM TRIS, 100 mM NaCl (adjusted at pH values between 3 and 10.5) at a concentration of 5 mg mL^{-1} for PEI, PSS, and PAH and 20 mg mL^{-1} for PGA and PLL.

The HSA was provided in concentrated solutions (200 mg mL^{-1}) for intravenous injection (prepared and purified by the Cohn method[13]) and further diluted to a concentration of 0.4 mg mL^{-1}.

Experimental Methods. *Optical Waveguide Light-Mode Spectroscopy (OWLS).* The buildup of polyelectrolyte multilayers (PEMs) and protein adsorption onto PEMs were followed in situ by OWLS.

OWLS is an optical technique based on the confinement of light in a high refractive index layer.[14] The core of the home-built experimental setup is an input grating sensor. This type of sensor makes use of the well-defined angle at which light couples into a waveguide by means of a grating coupler. The in-coupling equation gives the relation between certain discrete values of the θ_i angle between the laser beam and the normal to the grating and the effective refractive index N of the whole system:

$$N = \sin \theta_i + l\lambda/\Lambda \quad (1)$$

where l represents the diffraction order, equal to 1 in our experimental condition, λ corresponds to the wavelength of the light, and Λ is the grating constant.

On the high index film of a waveguide, a homogeneous, isotropic adlayer is adsorbed in a first step and covered by the solution present in the cell. In a second step, adsorption of an additional adlayer of different material is also possible. The change of optical parameters in the cover, for example, the thickness and refractive index of an adsorbed polyelectrolyte or protein adlayer, perturbs the evanescent field and leads to changes of the guided modes (N_{TE} and N_{TM}), highly sensitive for the changes of the refractive indices. By simultaneous measurement of two modes (p-polarized and s-polarized), the thickness and the refractive index of the adsorbed layer can be calculated.

The baseline values of the cell were determined in buffer before depositing the first polyelectrolyte layer. The buildup of the polyelectrolyte multilayer film was then performed as follows: First, PEI solution (5 mg mL^{-1}) was injected for 20 min. Then, progressively, architectures of PEI−PSS, PEI−PSS−PAH, and PEI−(PSS−PAH)$_2$ were built. Polyelectrolyte depositions were always separated by a 20 min long rinsing step. The buildup of the film was continued with the adsorption of the anionic PGA and the cationic PLL polypeptides until PEI−(PSS/PAH)$_2$−(PGA/PLL)$_3$ or PEI−(PSS/PAH)$_2$−(PGA/PLL)$_2$−PGA films were obtained.

HSA was then adsorbed on these multilayer films. The protein was allowed to adsorb from a continuous flow through the measuring cell (4 mL h^{-1}) for 1 h. Once the optical signals leveled off, the protein solution was replaced by buffer solution and desorption of the adsorbed proteins (if any) was monitored.

The experiments (both PEM construction and HSA adsorption) were performed at various pH values ranging from pH 3 to 10.5. HSA was adsorbed onto either positive (PLL) or negative (PGA) polyelectrolyte-terminated films.

OWLS data were analyzed by assuming that the polyelectrolyte multilayers behave as homogeneous and isotropic films. The additionally adsorbed proteins on the top of the polyelectrolyte multilayers were then analyzed using a homogeneous, isotropic bilayer model. The details of the data analysis were previously described.[8]

The measured N_{TE} and N_{TM} values depend on the refractive index profile of the film deposited on the oxide layer. The mode equations were resolved with no thin layer approximation,[8] and the structural parameters, that is, refractive index and thickness (n_A, d_A), of each deposited layer were obtained. The surface mass density, expressed in μg cm^{-2}, can then be calculated from the relation

$$\Gamma = (dn/dc)^{-1}(n_A - n_C)d_A \quad (2)$$

where dn/dc is the refractive index increment of the protein solution and n_C is the refractive index of the cover solution.

Atomic Force Microscopy (AFM). Contact mode images in liquid have been obtained with a Nanoscope III (Digital Instruments, Santa Barbara, CA). The silicon nitride cantilevers having a spring constant of 0.01 N/m have been silanized in order to facilitate visualization of charged polymers and protein. The hydrophobic tips were obtained by indirect vapor deposition of

(10) Shiratori, S. S.; Rubner, M. F. *Macromolecules* **2000**, *33*, 4213.
(11) Müller, M.; Brissova, M.; Rieser, T.; Powers, A. C.; Lunkwitz, K. *Mater. Sci. Eng., C* **1999**, *8*−*9*, 163.
(12) Müller, M. *Biomacromolecules* **2001**, *2*, 262.
(13) Cohn, E. J.; Hughes, W. L.; Weare, J. H. *J. Am. Chem. Soc.* **1947**, 1753.
(14) Tiefenthaler, K.; Lukosz, W. *J. Opt. Soc. Am. B* **1989**, *6*, 209.

a mixture made of 10 mL of bicyclohexane, 1−4 drops of octadecyltrichlorosilane (Aldrich), and 4−8 drops of carbon tetrachloride (Merck). The tips were incubated overnight in a closed chamber together with that mixture. Silanization allowed the imaging of either negative or positive surfaces. The polyelectrolyte multilayers were deposited on glass slides previously cleaned with 3% Hellmanex, 0.1 N HCl under heating, extensively rinsed with pure water, and dried under nitrogen. Layer-by-layer deposition of the PEI−$(PSS/PAH)_2$−$(PGA/PLL)_2$−PGA assembly was achieved in two separate steps. In the first step, until the PEI−$(PSS/PAH)_2$ level, the polyelectrolyte film was constructed by the deposition of 200 μL of polyelectrolyte solutions on the glass slide, leaving 15 min for adsorption. Each adsorption step was separated by a thorough rinse with buffer. In the second step, these slides were put into the liquid cell of the atomic force microscope, and the further construction of the polyelectrolyte architecture was achieved by flowing alternatively PLL and PGA through the liquid cell, intermediated by rinsing with buffer. In this way, in situ self-assembly of polypeptide films and imaging was realized, to avoid eventual aggregation problems that can be encountered due to insufficient washing when surfaces are prepared ex situ, as has already been pointed out in ref 15. AFM imaging of the PEM was performed at three pHs: 7.4, 8.5, and 9.5. After film imaging, HSA was adsorbed on the top of the multilayer films and further imaging was performed.

Height−friction mode images were scanned at a fixed scan rate (2 Hz) with a resolution of 512 × 512 pixels. The scan angle was chosen at 90 °C to increase sensibility. Several scans of each surface were performed in order to check the reproducibility of images and possible tip damages. Images were first taken on a $20 \times 20\ \mu m^2$ area then on a $5 \times 5\ \mu m^2$ area for higher resolution.

AFM images were analyzed by making profilometric sections. The cross-sections of the images in the *Z* direction, perpendicular to the scanning direction, provide the average surface roughness of the film, defined as $Ra = (1/n)\sum_{j=1}^{n}|Zj|$.

Fourier Transform Infrared (FTIR) Spectroscopy. FTIR spectroscopy was employed to check conformational changes within HSA induced by pH changes. Attenuated total reflectance FTIR (ATR-FTIR) spectra were measured with an Equinox 55 spectrophotometer (Bruker) on the surface of a ZnSe crystal using a liquid-nitrogen-cooled MCT detector. Single-channel spectra from 512 interferograms were calculated between 4000 and 400 cm^{-1} with 2 cm^{-1} resolution using Blackman-Harris three-term apodization and the standard Bruker OPUS/IR software (version 3.0.4). The analysis of the infrared spectra was carried out as in earlier work[16] using the SPSERV software (Dr. Cs. Bagyinka, Biological Research Center, Szeged, Hungary).

The FTIR experiments were performed in deuterated 25 mM MES, 25 mM TRIS, 100 mM NaCl buffer. HSA was adsorbed from a 0.4 mg mL^{-1} solution at pD 7.0 (the 0.4 unit shift between pH and pD was taken into account). The protein solution was circulated with a peristaltic pump above the ZnSe crystal until the adsorbed amount of the protein reached saturation (the process of the adsorption was followed by taking infrared spectra). Afterward, to remove the excess of non- or weakly bound protein, pure buffer was circulated above the ZnSe crystal. When needed, the pD of the system was changed to 3.0 and 10.0 by circulating the corresponding buffer above the protein assembly. Thus, the same adsorbed protein was measured at three different pD values.

Results and Discussion

Polyelectrolyte Film Formation in the pH Range 3.0−10.5. Multilayers were constructed as described in the experimental section, at eight pH values between 3 and 10.5. The biologically relevant PLL/PGA layer pairs were adsorbed on an underlying PEI−$(PSS-PAH)_2$ film, to decrease the eventual influence of inhomogeneity of the support surface. These polyelectrolytes are widely used in surface coatings as they form homogeneous, nanosized charged films on almost any kind of solid surface.

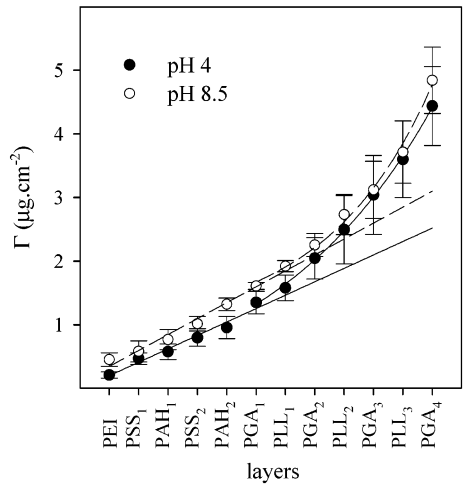

Figure 1. Typical layer-by-layer buildup of polyelectrolyte assemblies at pH 4 (●) and at pH 8.5 (○): the PEI, PSS, and PAH concentrations were 5 mg mL^{-1}; the PGA and PLL concentrations were 20 mg mL^{-1}. All polyelectrolytes were dissolved in 25 mM MES, 25 mM TRIS buffer containing 100 mM NaCl. The averages and the standard deviations were calculated from 4−12 experiments at each pH.

For two pH values, the buildup of PEI−$(PSS-PAH)_2$−$(PGA-PLL)_3$ multilayers as monitored by calculating the adsorbed mass from the N_{TE} and N_{TM} signals using the isotropic monolayer model is depicted in Figure 1. The growth of the film mass is linear in the PEI−$(PSS-PAH)_2$ regime and became exponential for $(PGA-PLL)_3$ deposition. The increase for this part was compatible with the exponential growth observed for other polyelectrolytes as well.[17] In Figure 1, the fitted linear and exponential curves are also given.

The exponential film growth mechanism was explained by an alternated "in" and "out" flow of the polyelectrolytes between the film and the solution. Once reaching the film surface, the out-flowing PLL or PGA will interact with their actual counterparts (PGA or PLL, respectively) arriving from the solution to the film surface. First, all freely diffusing components of the film form complexes with the polyelectrolyte arriving from the solution. Then, the polyelectrolyte being in large excess in the solution can diffuse toward the interior of the film. As a consequence, the amounts of the polyelectrolytes will be proportional to the thickness of the film; therefore an exponential film growth can be expected and was indeed found (Figure 1).

There are other examples for linear, superlinear, and exponential growth regimes in other systems. For PAC/PLL, nonlinear increase in the polymer assembly thickness was found at low salt concentration.[18] For PSS/PAH, the nonlinearity evolved with increasing salt concentration.[19] PLL/hyaluronic acid films also exhibited exponential growth at physiological salt concentration.[20]

The layer-by-layer increase of the adsorbed amount for the (PLL/PGA) films over the whole pH range (Figure 2) shows that at extreme pH values the rates of the buildups of the films were altered. The total adsorbed amounts of

(15) Menchaca, J. L.; Jachimska, B.; Cuisinier, F.; Pérez, E. *Colloids Surf., A* **2003**, *222*, 185.

(16) Schwinté, P.; Voegel, J.-C.; Picart, C.; Haikel, Y.; Schaaf, P.; Szalontai, B. *J. Phys. Chem. B* **2001**, *105*, 11906.

(17) Lavalle, P.; Gergely, C.; Cuisinier, F. J. G.; Decher, G.; Schaaf, P.; Voegel, J.-C.; Picart, C. *Macromolecules* **2002**, *35*, 4458.

(18) Yissar, V. P.; Katz, E.; Lioubashevski, O.; Willner, I. *Langmuir* **2001**, *17*, 1110.

(19) Ruths, J.; Essler, J.; Decher, G.; Riegler, H. *Langmuir* **2000**, *16*, 8871.

(20) Picart, C.; Mutterer, J.; Richert, L.; Luo, Y.; Prestwich, G. D.; Schaaf, P.; Voegel, J. C.; Lavalle, Ph. *Proc. Natl. Acad. Sci. U.S.A.* **2002**, *99* (20), 12531.

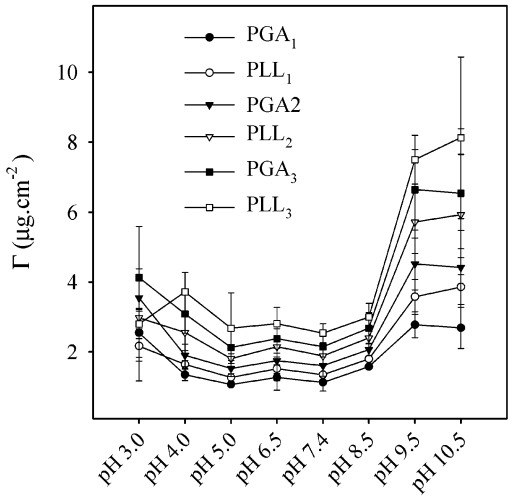

Figure 2. Evolution of the amount of the PGA or PLL taken up layer by layer as a function of pH. The lines are drawn just to guide the eyes. The averages and the standard deviations were obtained from 4−12 experiments at each pH.

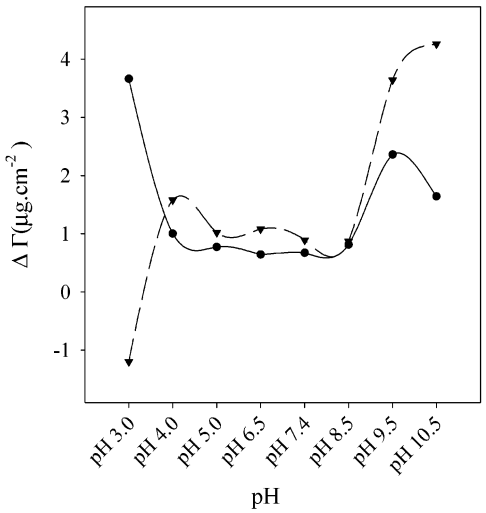

Figure 3. The increments of the adsorbed amounts of the $PLL_1 + PLL_2 + PLL_3$ (▼) polycation and the $PGA_1 + PGA_2 + PGA_3$ (●) polyanion layers as a function of pH.

the $(PGA/PLL)_3$ contributions varied between 3 and 8 $\mu g/cm^2$ in the pH range studied.

Since polyelectrolyte adsorption is primarily governed by electrostatic interactions, the degree of ionization of PGA and PLL when entering the films must be important. The pK_a values of PGA and PLL in solution are 4.9 and 9.8,[21,22] respectively. However, as often observed, the adsorption on a charged surface or multilayer architecture as well as the presence of ionic salt ions can strongly modify the local pK_a values.

Previous results of Yoo et al.[23] on PAC/PAH films may help to estimate the effect of the polyelectrolyte architecture on the pK_a values of the components. The pK_a of PAC, which was 5.5 in solution, dropped to 4.0 when PAC was in a polyelectrolyte film constructed in the absence of salt. When salt was present, the pK_a of the same carboxylic groups was 4.5. Taking into account these pK_a drops upon polyelectrolyte film forming, a local pK_a value for PGA in the film of about 4.0−3.5 can be assumed for our system. Recent experiments performed in FTIR spectroscopy in ATR mode suggested also an accentuated lowering (2 pH units) of PGA's pK_a compared to those obtained in solution (Schwinté, private communication).

Similarly, a pK_a drop from 10.5 in solution down to 9.8 was found comparing lysine with PLL.[22] Moreover, PLL adsorption onto a negatively charged surface (PGA) can be accompanied by a proton release from NH_3^+ groups leading to a further drop of the effective pK_a value. Figure 2 shows that the largest polymer depositions are observed at low (3.0−4.0) and high (9.5−10.5) pH values, where one of the polyions is only partly charged. At the most extreme pH values of 3 and 10.5, (PLL/PGA) multilayer buildups were less reproducible. At high pH values, the charge neutralization of the fully ionized PGA molecules needs the adsorption of higher amounts of only partly ionized PLL molecules, which, thus, may form large loops. The resulting PLL surface increases may lead in the following to larger PGA uptake (a similar phenomenon was observed by Shiratori[10] for the PAC/PAH system). The excess charges of the fully ionized PGA molecules can be compensated by the uptake of small cations (from the high ionic strength of our medium).

This effect is documented in Figure 3 showing at high pH values larger uptakes of both PGA and PLL.

For the intermediate pH values (pH 5−8.5) where both polyions are totally or highly ionized, the total adsorbed amount of polyions is stable and it has at least 0.5 nm thickness per layer, having an adsorbed mass of 0.26 $\mu g\ cm^{-2}$ in the average of 3 layers.

At low pH, where PLL is totally and PGA only partly ionized, the same ion-pair interactions but in the opposite sense as for high pH should govern the film buildup. We could however less demonstrate it in this pH domain (Figure 2). At pH 3, each PLL injection induces a loss in the adsorbed amount (Figure 3). Film deposition and growth continue still because part of the PGA remains on the surface (PLL induces only partial PGA desorption).

The different buildup of the PLL/PGA films at extreme pH values (Figures 2 and 3) can involve additional mechanisms as well. Besides ionic interactions, at extreme pH values, hydrogen bonding can play an important role in the film buildup. This is imaginable if one considers the structures of PGA and PLL. At high pH, the acidic COO^- groups of PGA, besides their charges, are able to make H-bonds as well with the neutral N−H groups of the PLL, while at low pH the extra H giving the positive charge to PLL may interact mainly with the C═O part of PGA's COOH group, the OH group will repulse it. Therefore, one may expect larger buildup increases at high pH values as compared to those at low pH, as experimentally observed (Figures 2 and 3).

As regards the overall pH dependence of the buildup of the polyelectrolyte films, the phenomenon described above seems to constitute a more general mechanism as well as in the presence or absence of ionic salts. Thus, for a different system (PAC/PAH), in the absence of salt, Rubner et al.[10,23] similarly found that the incremental increases for both polyions were minimal when the two polyelectrolytes were fully ionized. Reversely, the increases of the incremental thickness for both polyions became larger when one of the polyions was partly charged.

HSA Adsorption. *OWLS Measurements.* Adsorption of HSA was performed over the same pH range, either on PGA- or PLL-terminated films. The adsorbed HSA amounts could be evaluated by means of monolayer or bilayer models. Previously, by comparing OWLS and

(21) Cheng, Y.; Corn, R. M. *J. Phys. Chem. B* **1999**, *103*, 8726.
(22) Cantor, R.; Schimmel, P. R. *Biophysical Chemistry*; W. H. Freeman: San Francisco, 1980.
(23) Yoo, D.; Shiratori, S. S.; Rubner, M. F. *Macromolecules* **1998**, *31*, 4309.

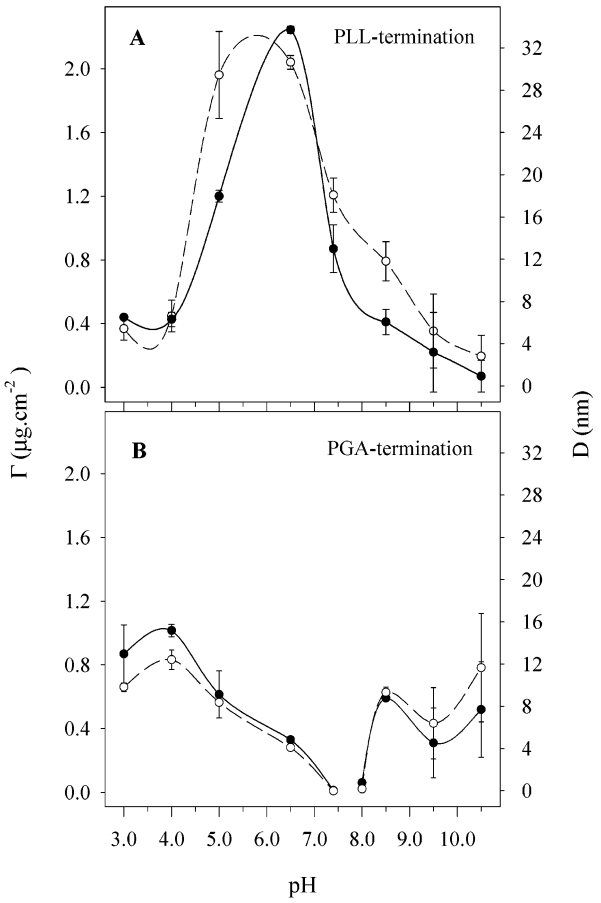

Figure 4. Evolution of adsorbed amounts (●) and of the thickness (○) of HSA on polyelectrolyte films terminated by a polycationic PLL layer (A) or by a polyanionic PGA layer (B) as a function of the pH. HSA was adsorbed from a 0.4 mg mL^{-1} solution dissolved in 25 mM MES, 25 mM TRIS, 100 mM NaCl. The averages and the standard deviations were obtained from 2−6 experiments at each pH. The lines are drawn just to guide the eyes.

scanning angle reflectometry (SAR) data the results for the adsorbed amounts for HSA obtained by using either the mono- or the bilayer model[8] differed by 20%. It has been recognized that the theory of optical invariants developed for the analysis of SAR data[24] gives a clue as to which model should be used.[8] SAR measurements performed on HSA adsorption onto (PSS/PAH) polyelectrolyte films (at pH 7.4) demonstrated that the protein layer should be considered as a second layer, that is, the bilayer model should be used for the calculations.[9]

On this basis, we will discuss here only the results obtained with the bilayer model. Figure 4A shows the thickness and the amount of HSA adsorbed onto PLL-terminating films as a function of the pH.

In Figure 4B, the same data are depicted for PGA-terminated films. Data points represent averages of 2−6 measurements at each pH. Generally, larger amounts of HSA were adsorbed onto the PLL-terminated films (0.1−2.2 μg cm^{-2}) as compared with the PGA-terminated ones (0.02−0.88 μg cm^{-2}).

In previous studies, restricted to the physiological pH 7.4 value, it was found that more HSA was adsorbed when the protein and the terminating layer of the polyelectrolyte film were oppositely charged,[9,25,26] pointing to the primary importance of electrostatic forces in the protein adsorption mechanism.

When HSA adsorption is studied over a wide pH range as in our case, the net charge of HSA will also change with the pH. The pH_i value of HSA is 4.6. Below this pH, HSA has a net positive charge, and above it, a net negative charge.

Even taking the actual charge of HSA into account, its adsorption is not a trivial function of the pH as can be seen in Figure 4A,B. (Data were less reproducible at extreme pH values, mainly at the basic ones (pH 9.5−10.5) probably due to the lower ionization of the underlying PLL.) HSA adsorption onto the positive PLL layer is maximal at intermediate pH values, 5.0−8.5, whereas on the negative PGA layer the highest adsorptions were found at extreme pH values: 3.0−4.0 and 8.5−10.5 (Figure 4A,B).

HSA adsorption on PLL reaches a maximal value (2.2 μg cm^{-2}) at pH 6.5, where the interactions between the positively charged polypeptide and the protein bearing negative charges become optimal (Figure 4A). At pHs lower than pH 4.6, HSA starts to be positively charged, and it thus adsorbs in smaller quantities on the positive-ending films. At high pH values where PLL becomes less ionized, the interactions between PLL and the negatively charged HSA are also diminishing. It is not clear, however, why the decrease of the HSA adsorption starts already at pH 6.5 since PLL remains rather strongly positively charged at least up to about pH 8.5. A possible origin of this observation based on FTIR and AFM data will be presented later on.

HSA adsorption onto PGA-terminated films is highest at pH values below 4.6 where HSA is globally positively charged (Figure 4B). As also expected, at pH values above the isoelectric point of HSA, the repulsive interactions between the protein and PGA, both being negatively charged, lead to a decrease in thickness and deposited amount. Around physiological pH values, HSA adsorption becomes practically insignificant. Similar observations were previously made for the (PGA/PLL) system at pH 7.4 in contact with serum proteins[27] and for albumin with films containing weak polyanions such as poly(acrylic acid) or poly(maleic acid−propylene).[28,29]

The increasing adsorption of HSA onto PGA-terminated films above pH 8.0, however, is unexpected since at these pH values both PGA and HSA are highly negatively charged. The significant amounts of HSA adsorbed above pH 7.4 in particular on PGA-terminated films could be related to the α-helical content of HSA. α-Helical structures are very compact and highly ordered, involving numerous ion-pair interactions between charges masked in their interiors.[22] Therefore, α-helices exhibit very few if any free charges on their surfaces as compared to other kinds of secondary structures. Thus, a decrease in α-helix content when pH changes from 7.4 to 8.5 if it would exist could lead to more accessible (not necessarily negative) charges of HSA, available for interaction with PGA, despite both of them being strongly negatively charged at these pH values.

FTIR Measurement. To have deeper insight to what is happening with the secondary structure of HSA as a

(24) Mann, E. K.; Heinrich, L.; Voegel, J. C.; Schaaf, P. *J. Chem. Phys.* **1996**, *105*, 6082.
(25) Khopade, A. J.; Caruso, F. *Langmuir* **2003**, *19*, 6219.
(26) Ladam, G.; Schaad, P.; Voegel, J. C.; Schaaf, P.; Decher, G.; Cuisinier, F. J. G. *Langmuir* **2000**, *16*, 1249.
(27) Richert, L.; Lavalle, Ph.; Vautier, D.; Senger, B.; Stoltz, J.-F.; Schaaf, P.; Voegel, J.-C.; Picart, C. *Biomacromolecules* **2002**, *3*, 1170.
(28) Müller, M.; Rieser, T.; Kothe, M.; Kesler, B.; Brissova, M.; Lunkwitz, K. *Macromol. Symp.* **1999**, *145*, 149.
(29) Müller, M.; Rieser, T.; Dubin, P. L.; Lunkwitz, K. *Macromol. Rapid Commun.* **2001**, *22*, 390.

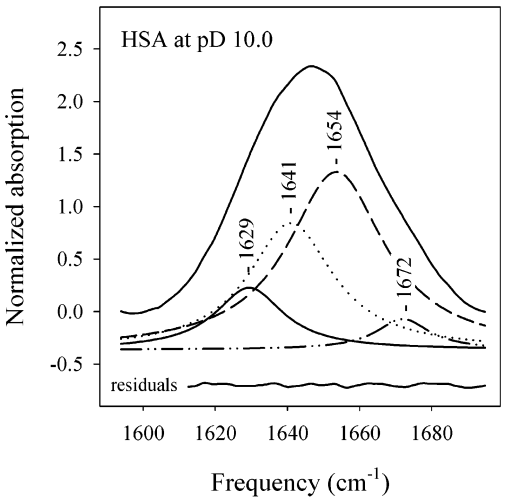

Figure 5. Amide I′ band of HSA adsorbed onto PGA/PLL multilayers measured at pD 10.0 by ATR-FTIR spectroscopy and its decomposition into Gaussian-shaped component bands. The quality of the fit is shown at the bottom by the residuals. Assignments of the component bands are given in the text, and their variations with pD are depicted in Figure 6.

function of pH, we performed FTIR spectroscopy in ATR mode in a deuterated environment at pD 3.0, 7.0, and 10.0. For detailed information, the amide I′ band of the protein (1700−1600 cm^{-1}) was analyzed.

This region has been extensively studied and used in connection with the determination of the secondary structure of proteins. The amide I region is very complex; it contains several overlapping component bands assignable to different secondary structure elements of the protein. Therefore, several techniques were used to extract as much information as possible from the region. The problem with the use of second derivatives[30] or Fourier self-deconvolution[31] for resolution enhancement is that they are very sensitive to noises (e.g., water-vapor bands). For a discussion on the applicability and limitations of the above resolution-enhancement techniques, see the reviews in refs 32 and 33. Since reaching a proper signal-to-noise ratio might be a problem even in the case of dissolved proteins, and in our case the adsorbed proteins' absorptions were in the range of a few mOD, we could not reach the signal-to-noise ratios required for the use of these techniques. The arbitrary absorption units up to 2.5 shown in Figures 5 and 6 were obtained by a normalization procedure, in which the spectra in the 1700−1600 cm^{-1} region were divided by their average absorptions over the same region. This normalization for the total intensity of the band was chosen because normalization to the maximum absorption could lead to erroneous relative component band intensities.

To remain credible, our approach aimed for fitting the amide I′ region of the infrared spectrum with the minimum number of amide I′ component bands. Concerning the heterogeneity of our system, Gaussian-shaped components were chosen to fit the measured infrared spectrum (for details of the fitting procedure, see the Appendix of ref 16).

The result of such decomposition is shown for a HSA FTIR spectrum taken at pD 10.0 in Figure 5. It can be seen from the residuals depicted at the bottom of Figure 5 that very good fits could be obtained. All together four component bands had to be assumed for fitting the amide I′ region of HSA infrared spectra taken at three different pD values. The component at around 1629 cm^{-1} was attributed to intermolecular β-sheet structures, whereas the band whose frequency varied between 1634 and 1641 cm^{-1} was assigned to intramolecular β-sheets. (Actually, the shift toward higher frequencies of this component band may indicate the appearance of some nonordered structures as well, but the signal-to-noise ratio of the experiments did not allow a confident resolution of an additional band.) The components found at 1651−1653 cm^{-1} and 1672−1673 cm^{-1} correspond to α-helices and turn structures, respectively.[16] The three major components characteristic to a given secondary structure are depicted for HSA at pD 3.0, 7.0, and 10.0 in Figure 6A−C.

We found that the α-helix content decreased, whereas the intramolecular β-sheet content increased for the extreme pH values and the change was larger for the alkaline pH values (Figure 6B,C). In addition, at pD 10.0 we found a considerable amount of intermolecular β-sheets (Figure 6A). The presence of this intermolecular β-structure could be the consequence of the HSA−ZnSe crystal interaction but could also indicate protein self-aggregation. It may also be relevant for HSA−polyelectrolyte interactions as well, in the sense that the protein structure can be sufficiently perturbed for a large rearrangement at pD 10.0 after adsorption.

These infrared spectroscopic results are in agreement with those of far-UV CD measurements of Dockal et al.[34] showing a decrease of the α-helix content in HSA between pH 7.4 and 9.0. Infrared spectroscopic measurements in the pH range 5.0−3.0 also showed the loss of α-helix content.[35]

At high pH, as we have shown, there is a considerable decrease of the α-helix content in HSA (Figure 6C), which may render accessible local charges, capable of maintaining HSA adsorption onto PGA (Figure 4B). For PLL-terminated films, the increase in α-helical content when pH goes from 6.5 to 7.4 could lead to the observed decreased amount of adsorbed HSA. At higher pH values, the change in the ionization of PLL (it becomes less ionized) overwrites the possible effect of the protein structural change and led to the observed decrease in HSA adsorption (Figure 4A).

Lowering the pH to 3 also caused a decrease of the α-helix and an increase of the β-sheet content in HSA. For PGA-terminated films, accordingly, the adsorbed amounts of HSA increased lowering the pH from 6.5 to 4.6 in a range where both PGA and HSA are negatively charged. For PLL-terminated films, the same structural change of the protein may help HSA adsorption, in the pH range 7.4−5.0. Further lowering the pH, albumin starts to bear positive charges; thus its adsorbed amount is reduced.

Our results indicate that the actual protein conformation can strongly interfere in its adsorption onto charged surfaces.

Atomic Force Microscopy. To investigate also a possible film morphology origin of the higher HSA adsorption onto the PGA-terminated films at alkaline pH, we studied the film surfaces with AFM in the pH range 7.4−9.5. We found increasing rugosity with increasing pH (Figure 7). Film surface roughness (Ra) calculated on 5 × 5 μm^2 scanning

(30) Byler, D. M.; Susi, H. *Biopolymers* **1986**, *25*, 469.
(31) Kauppinen, J. K.; Moffat, D. J.; Mantsch, H. H.; Cameron, D. G. *Appl. Spectrosc.* **1981**, *35*, 271.
(32) Surewicz, W. K.; Mantsch, H. H. *Biochim. Biophys. Acta* **1988**, *952*, 115.
(33) Surewicz, W. K.; Mantsch, H. H.; Chapman, D. *Biochemistry* **1993**, *32*, 389.
(34) Dockal, M.; Carter, D. C.; Rüker, F. *J. Biol. Chem.* **2000**, *275*, 3042.
(35) Murayama, K.; Wu, Y.; Czarnik-Matusewicz, B.; Ozaki, Y. *J. Phys. Chem. B* **2001**, *105*, 4763.

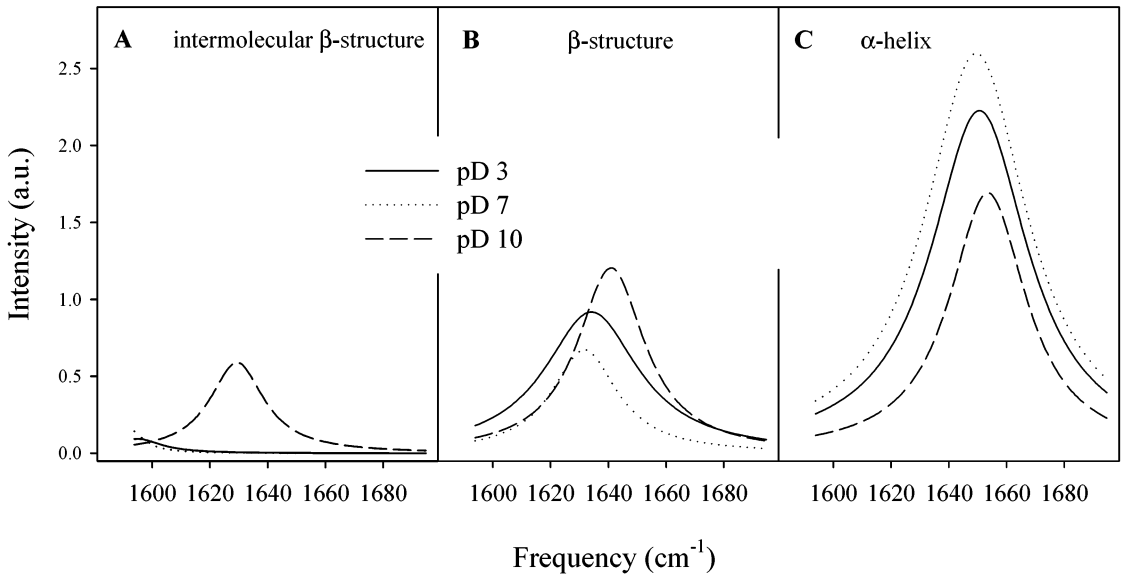

Figure 6. Component bands obtained from the fits of amide I bands of the ATR-FTIR spectra of HSA adsorbed onto a ZnSe internal reflection element at pD 3.0, 7.0, and 10.0. The amide I′ bands were normalized before decomposition; thus the intensities depicted here are directly comparable. The assignments are as follows: (A) (1629 cm^{-1}) intermolecular β-sheets; (B) (1634−1641 cm^{-1}) intramolecular β-sheets; (C) (1651−1653 cm^{-1}) α-helix.

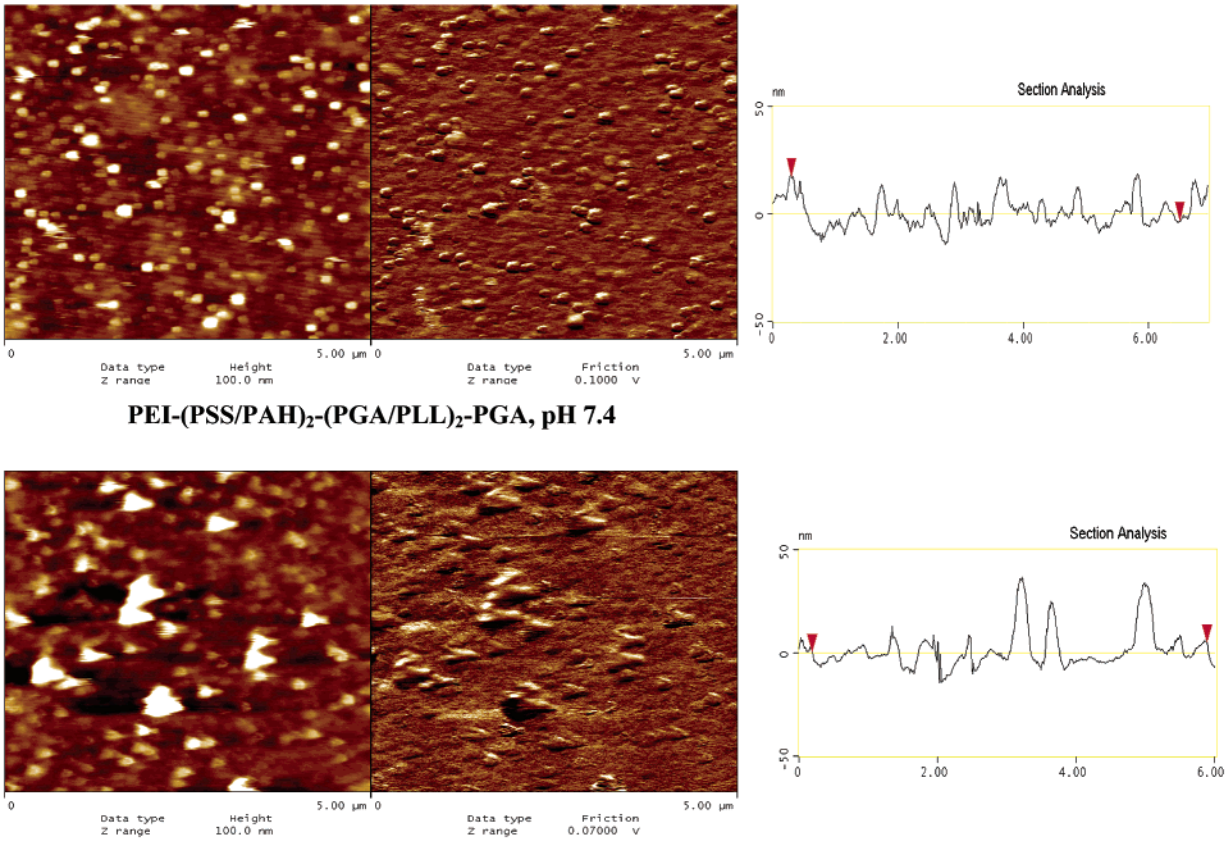

Figure 7. Surface topography and profilometric sections of PEI−$(PSS/PAH)_2$−$(PGA/PLL)_2$−PGA layers at pH 7.4 and 8.5, taken by in situ liquid cell AFM in contact mode on $5 \times 5\ \mu m^2$ areas. Experimental conditions were the same as for the OWLS measurements.

areas increased from 4.9 (±0.5) nm for pH 7.4, to 8.9 (±1.1) nm at pH 8.5, and to 22.0 (±2.3) nm at pH 9.5. At high pH values, PLL is only partly ionized, and that may cause incomplete charge compensation when adsorbed on the previous, oppositely charged layer, leading to formation of granulates at the interface. The charge decrease of the PLL molecules above pH 8.5 could lead to weaker surface binding and thus to surface clustering.

Previously, similar grain formations were observed at pH 10.5 for PSS/PAH self-assemblies and were attributed to the complex formation of the two polyelectrolytes.[15] Neutron reflectometry has already shown that polyelectrolyte films can be strongly interdigitated,[36] and there is

(36) Losche, M.; Schmitt, J.; Decher, G.; Bouwman, W. G.; Kjear, K. *Macromolecules* **1998**, *31*, 8893.

also other evidence that polyelectrolytes form complexes inside the multilayer.[37] To elucidate this point, recently a theoretical model has been proposed.[38]

The granulate structures observed by us in AFM at high pH should be related to the sizes of the complexes formed if positive and negative polyelectrolytes were mixed in solution. According to previous studies performed at pH 8.4, PLL and PGA form complexes and their structure is very similar in polyelectrolyte films and in solution.[39]

We suggest that the granular structure observed at pH 8.5 is the result of the formation of PLL−PGA complexes. Such complexes can destroy the layered structure of the polyelectrolyte films and may provide access to positive charges for HSA even if the uppermost layer is PGA.

Unfortunately, direct observation of HSA deposition by AFM is not possible, as on such rough surfaces and granulated structures the distinction between the small (69 kDa) globular HSA molecules and the also globular PLL/PGA complexes is very difficult.

Nevertheless, an indirect proof of protein deposition can be found if one compares roughness before and after adsorbing HSA on PGA-ending films. After protein adsorption, on $5 \times 5\ \mu m^2$ images, the Ra values remained unchanged at around 4.9−4.6 nm at pH 7.4 but increased from 8.9 to 10.6 nm at pH 8.5 and from 22.0 to 26.8 nm at pH 9.5. This indicates a correlation between film surface roughness before and after HSA adsorption and suggests a relation between the amount of the uptaken protein and film rugosity. This effect, together with a decrease of the α-helix content in HSA, could be the reason for the unexpected HSA uptakes at high pH values.

The high amounts of HSA adsorbed onto PLL-ending film in the intermediate pH range remains to be explained. From the amount of adsorbed proteins, the surface coverage can be estimated. At pH 7.4, native HSA can be schematically represented as a prolate ellipsoid,[40] with characteristic dimensions of $12 \times 2.7 \times 2.7\ nm^3$. The molecule exhibits a positive domain at one extremity and two negative domains at the other one; it carries a net −15 charge (in units of the elementary charge *e*). Assuming that the molecules are adsorbed in "end-on" configuration, one gets 144% coverage for HSA adsorbed on PLL at physiological pH. For a "side-on" conformation, we calculated a surface coverage of 641%. Both of these coverages are far above the expected jamming limit for elongated ellipsoids.[9] It is thus expected that more than monolayer adsorption is found. There are no available models for the protein at other pHs, but if we assume that a change of the pH from 7.4 to 6.5 does not perturb the molecule too much, one can notice even higher surface coverage on PLL at 6.5. Here the thickness of the adsorbed protein layer is 32 nm, 3 times larger than the long axis of the protein ellipsoid.

Comparable observations were made for HSA adsorption onto PSS/PAH architectures, when HSA adsorbed in end-on configuration in more than three layers onto the positively charged PAH-terminated film.[9]

Two explanations were previously advanced for HSA adsorption. Thick protein layers can result from cooperative attractive interactions between the negative extremity of the protein and the positively charged surface of a polyelectrolyte multilayer. The first protein layer adsorbed in such a way exhibits a net positive surface charge, which again acts as an attractive surface for further proteins from the solution. However, as the process evolves, the protein layer becomes less structured so that the surface excess charge decreases and the process ends. Protein adsorption in such a way would be the result of the interplay between transport and reorganization. In a second mechanism, protein molecules would be somehow entangled in the polyelectrolytes of the outer layer, leading to the outermost mixed polyelectolyte/protein architecture with possible thicknesses larger than a monolayer. This second process appears to be more probable for the soft, PGA/PLL-terminated films.

Conclusions

The buildup of weak polyionic multiassemblies and adsorption of the model human serum albumin protein was studied in the pH range 3−10.5. Optical waveguide light-mode spectroscopy and liquid cell atomic force microscopy in contact mode were employed to follow adsorption in situ of polypeptides and human serum albumin and to provide structural information about the surfaces. Fourier transform infrared spectroscopy revealed conformational changes induced by pH variations in HSA.

The pH dependence of multilayer buildup and protein adsorption was not straightforward. Films constituted by weak polyelectrolytes are very sensitive to the pH of the solution, since ionization varies with pH, especially below or above the pK_a values of the polyions. This study shows that by changing the pH one can more strongly influence the thickness of the adsorbed polyelectrolyte PGA/PLL layers than by the often used ionic strength variations.

The present investigation highlights the influence of the pH on the structure of films built from weak polyelectrolytes even in the presence of physiological salt concentrations. Concerning protein uptake at pH 7.4, HSA adsorbs onto the oppositely charged PLL layer, but the negative PGA surface fully prevents its adsorption.

In general, protein adsorption is largely dependent upon the charge of the terminating layer of the multiassembly. There is an interplay between the pH_i of the protein and the pK_a values of PGA and PLL. In addition, structural changes in the film, leading to large polypeptide aggregates, and pH-induced structural changes in the protein can modify the adsorbed protein amount.

Acknowledgment. This work was supported by the SIMI project (GRDI-2000-26823) financed by the European Commission, the Franco-Hungarian bilateral cooperation (Balaton, F-2/01), by the Hungarian Science Foundation (OTKA T031973), and by the ACI program (ACI: Technologies pour la Santé) from the French Ministry of Research. We also thank Pascale Schwinté for valuable discussions and Cosette Betscha for help in experimenting.

LA049932X

(37) Li, M.; Schlenoff, J. B.; Ly, H. *J. Am. Chem. Soc.* **1998**, *120*, 7626.
(38) Castelnovo, M.; Joanny, J.-F. *Langmuir* **2000**, *16*, 7524.
(39) Boulmedais, F.; Scwinté, P.; Gergely, C.; Voegel, J.-C.; Schaaf, P. *Langmuir* **2002**, *18*, 4523.
(40) Haynes, C. A.; Norde, W. *Colloids Surf., B* **1994**, *2*, 517.